

Dynamics and robustness of familiarity memory

J.M. Cortes¹, A. Greve, A.B. Barrett and M.C.W. van Rossum

Institute for Adaptive and Neural Computation

School of Informatics, University of Edinburgh

5 Forrest Hill, Edinburgh EH1 2QL, UK

1. Correspondence to: Jesus M. Cortes. email: jcortes1@inf.ed.ac.uk

Abstract

When one is presented with an item or a face, one can sometimes have a sense of recognition without being able to recall where or when one has encountered it before. This sense of recognition is known as familiarity. Following previous computational models of familiarity memory we investigate the dynamical properties of familiarity discrimination, and contrast two different familiarity discriminators: one based on the energy of the neural network, and the other based on the time derivative of the energy. We show how the familiarity signal decays after a stimulus is presented, and examine the robustness of the familiarity discriminator in the presence of random fluctuations in neural activity. For both discriminators we establish, via a combined method of signal-to-noise ratio and mean field analysis, how the maximum number of successfully discriminated stimuli depends on the noise level.

Keywords: Recognition memory, Familiarity discrimination, Storage capacity.

Abbreviations: SNR, Signal-to-Noise Ratio; FamE, Familiarity discrimination based on Energy; FamS, Familiarity discrimination based

on Slope.

Introduction

Recognition memory is supported by at least two different types of retrieval processes: recollection and familiarity. While recollection requires detailed information about an experienced event, familiarity just distinguishes whether or not the stimulus was previously encountered. A well known example is the encounter with a colleague during a conference: one might recognize the person, but fail to remember the time and place of an earlier meeting.

Familiarity memory is thought to have a very large capacity. In the early 1970s, Standing and collaborators (Standing, 1973) tested the capacity in humans by presenting participants with a large number (10,000) of images. Surprisingly, after this one-shot learning, participants were able to successfully recognize most of the previously seen pictures, suggesting that the capacity of recognition memory for pictures is very large indeed.

Experimental psychologists have formulated *dual-process* theories which characterize the precise contribution of familiarity and recollection to recognition memory, for a review see (Yonelinas, 2002). Anatomically, researchers have proposed that different brain areas are engaged during recollection and familiarity processing. Single item familiarity is believed to be processed in the perirhinal cortex, whereas recollection is believed to engage the hippocampus, for a review see (Brown and Aggleton, 2001). Furthermore, electro-physiological studies using single cell recordings in monkeys and rats (Brown et al., 1987; Brown and Xiang, 1998) report that about 30 percent of neurons in the perirhinal cortex show increased activity after presenting new compared to old stimuli. These neurons have been interpreted

as novelty detectors. However, this association between the memory processes and brain area is still unclear and seems to depend on the nature of the stimulus (Aggleton and Brown, 2005; Rugg and Yonelinas, 2003).

Recent neuroimaging studies using, for example, event-related potentials (ERPs) (Rugg and Yonelinas, 2003), have revealed that familiarity and recollection have distinct temporal characteristics. Familiarity is linked to a frontal ERP modulation that occurs around 300-500ms post-stimulus presentation, whilst recollection is thought to evoke a parietal ERP modulation around 500-800ms after stimulus presentation (Rugg et al., 1998; Greve et al., 2007). Therefore, the speed of processing of familiarity discrimination is more rapid than recollection. Behavioral experiments provide further evidence for this: if only very limited time is available for a recognition decision, participants rely primarily on familiarity as opposed to recollection processes (Doshier, 1984).

In the field of computational neuroscience, modeling of recollection via attractor neural networks has a long history using auto-associator Hopfield networks (Hopfield, 1982; Amit, 1989). Familiarity discrimination has only been studied much more recently (Bogacz and Brown, 2003). Computational models of familiarity discrimination have a much higher storage capacity for recognition than associative memory networks that perform associative recall. For a wide range of conditions, Bogacz et al. showed that the maximum storage is proportional to the number of synapses within the network (Bogacz and Brown, 2003). This is much larger than the capacity to recall, which is proportional to the square root of the number of synapses (i.e. the number of neurons in a fully connected network) (Amit, 1989). Intuitively this is easily understood; familiarity needs to store just a single bit (familiar versus non-familiar) per pattern, whereas to recall an event

requires the retrieval of the whole pattern (pattern completion).

In this paper we study how the dynamics of the network affects familiarity discrimination. We compare two different familiarity discriminators: familiarity based on Energy, FamE, which was previously introduced by Bogacz et al (Bogacz and Brown, 2003), and a familiarity discriminator which is the time derivative of FamE (Hopfield, 1982). From here on, we will call this latter discriminator the slope, and label it FamS.

We show in our model how the signal for both familiarity discriminators decays very quickly after stimulus presentation, in concordance with the results from neuroimaging (Rugg et al., 1998; Greve et al., 2007). In addition, to investigate the robustness of familiarity detection, we study how it is affected by random fluctuations that are ubiquitously present in the nervous system. As in models of attractor neural networks (Amit, 1989), this external source of noise is taken to be independent of the learned patterns and is controlled by a *temperature* parameter.

Two familiarity discriminators

We consider a network of N binary neurons, each with an activity $s_i(t) = \pm 1$, the two states corresponding respectively to firing and not firing. The complete network activity is characterized by $\mathbf{s}(t)$. Any two neurons are connected by synaptic weights w_{ij} . As standard in artificial network models, the network has a learning phase in which it encodes M stimuli $\mathbf{x}^\rho \equiv \{x_i^\rho\}_{i=1}^N$ ($\rho = 1 \dots M$) in its weights using a Hebbian learning rule

$$w_{ij} = \frac{1}{N} \sum_{\rho=1}^M x_i^\rho x_j^\rho. \quad (1)$$

It can be shown that this learning rule is optimal in the limit of large N, M (unpublished results). During the subsequent test phase, the network's performance is evaluated. At $t = 0$, the probe stimulus $\hat{\rho}$ (which is either a familiar or novel stimulus) is loaded into the network, $\mathbf{s}(t = 0) = \mathbf{x}^{\hat{\rho}}$.

To define the network dynamics we assume that each neuron is updated precisely once, probabilistically and asynchronously, in each unit of time. (The exact duration that a time unit in the model corresponds to is hard to extract by comparing the model to, say, ERP data given the additional delays present in the biology, but it should probably be on the order of 10..100ms.) As standard in artificial neural networks, and in analogy with magnetic systems in physics, the random fluctuations are controlled by a temperature parameter T . These so-called Glauber dynamics have been extensively studied in many different stochastic systems, for instance (Marro and Dickman, 1999). The probability distribution, after update, is given then by

$$P\{s_i(t+1) = \pm 1\} = \frac{1}{1 + \exp[\mp 2\beta h_i(t)]}, \quad (2)$$

where $\beta \equiv 1/T$ is the inverse temperature parameter, and $h_i(t) \equiv \sum_{j=1}^N w_{ij}s_j(t)$ is the total presynaptic current to the neuron i . Accordingly, for low temperature, the noise is small and there is a strong positive correlation between the input current h_i and the output s_i , whilst for high temperature the output of a node is dominated by noise and is more or less independent of its input.

The energy in the network at time t is defined as

$$E(t) \equiv - \sum_{ij} w_{ij} s_i(t) s_j(t). \quad (3)$$

As was previously reported in (Bogacz and Brown, 2003), the energy $E(t = 0)$ is able to effectively discriminate between old and novel stimuli. As we explain later, this energy is of order $-(N + M)$ for learned stimuli, but of order $-M$ for novel stimuli. Consequently, the energy or familiarity for old and novel stimuli are macroscopically different (they differ by order N , while the std.dev.= $\sqrt{2M}$) and the difference can thus be used as a familiarity discriminator. We call this discriminator FamE.

However, the use of the energy is only one possible approach to model familiarity discrimination. The time derivative, or slope, of the energy $S = \frac{dE(t)}{dt}$ can also be used as a familiarity discriminator. It indicates how quickly the network's energy changes, when either a novel or old stimulus is presented. Interestingly, this familiarity measure was originally proposed by Hopfield in his seminal 1982 paper (Hopfield, 1982), but to the best of our knowledge it has never received further exploration. We call this discriminator FamS.

For convenience, we shall express the energy and the slope as functions of the M -dimensional vector $\mathbf{m}(t) \equiv \{m^\rho(t)\}_{\rho=1}^M$, the overlaps between the current network activity and each of the stored patterns. The components of this overlap vector are defined by

$$m^\rho(t) \equiv \frac{1}{N} \sum_{i=1}^N x_i^\rho s_i(t). \quad (4)$$

Assuming the Hebbian learning rule (1), the energy (3) in terms of the overlaps is given by

$$E(t) = -N \sum_{\rho=1}^M [m^\rho(t)]^2, \quad (5)$$

whilst the slope (first derivative of the energy) is given by

$$S(t) = -2N \sum_{\rho=1}^M m^{\rho}(t) \frac{dm^{\rho}(t)}{dt}, \quad (6)$$

and is thus proportional to the time derivative $dm^{\rho}(t)/dt$ of the overlaps.

Dynamics of familiarity discrimination

To mathematically address the network dynamics we assume the mean field approximation, i.e. $s_i \approx \langle s_i \rangle$. Under this approximation one obtains from equation (2), the dynamical equations for the overlaps (4):

$$\frac{dm^{\rho}(t)}{dt} = -m^{\rho}(t) + \frac{1}{N} \sum_{i=1}^N x_i^{\rho} \tanh[\beta \sum_{\nu=1}^M x_i^{\nu} m^{\nu}(t)]. \quad (7)$$

The mean field formulation provides an accurate description of the dynamics of the system provided the temperature is not too high (see below).

Knowing the dynamics, we focus on the time evolution of the two discriminators, energy and slope, defined in the previous section. To measure the temporal persistence, Figure 1 illustrates the time evolution of FamE and FamS when tested with novel or old stimuli. We compare the time evolution by simulations with Glauber dynamics given by equation (2), and by using the mean field dynamical equations (7).

(FIGURE 1 HERE)

Figure 1 A and B, shows how the energy associated with old stimuli is much lower than for new stimuli. However, after a short transient of 4-5 units of time, both signals become similar to each other, i.e. familiarity discrimination based on energy deteriorates rapidly post stimulus presentation.

Like the energy, the slope also shows a transient signal when the network is presented with a novel vs old stimulus, figure 1 graphs C and D. For low temperature, the slope for old stimuli is practically zero. This can be easily interpreted. An old stimulus corresponds to one of the local minima (attractors) of the energy landscape. Because the temperature is low, and therefore the system is not receiving any external perturbation, the energy does not change, and its time derivative is practically zero. Similar to the energy, the slopes associated with old and new stimuli show significant differences immediately after stimulus presentation, but this difference diminishes shortly thereafter.

Summarizing, both discriminators can distinguish old from new stimuli immediately after stimulus presentation, but after a very short transient (of the order of five time units), the discrimination ability disappears. The slope tends to zero as time progresses because the network evolves towards a fixed point and becomes stationary (i.e. $S \approx 0$). Though measures to discriminate spurious from non-spurious attractor states have been proposed (Robins and McCallum, 2004), such measures do not directly translate into a discrimination between old and novel stimuli.

Robustness of the familiarity discriminators

To examine the performance of the two familiarity discriminators introduced in the previous section, we quantify the discriminability between the network responses to either new or old stimuli by the signal-to-noise ratio (SNR). Assuming two Gaussian probability distributions, $\mathcal{N}[\mu_{\text{new}}, \sigma_{\text{new}}^2]$ and

$\mathcal{N}[\mu_{\text{old}}, \sigma_{\text{old}}^2]$, associated with new and old stimuli, we define

$$\text{SNR} = \frac{|\mu_{\text{new}} - \mu_{\text{old}}|}{\sqrt{\frac{1}{2}\sigma_{\text{new}}^2 + \frac{1}{2}\sigma_{\text{old}}^2}}. \quad (8)$$

To check that the distributions are indeed Gaussian, we repeated the simulation of Fig. 1 100 times and computed the probability distributions. For both FamE and FamS the 4th moments of their distribution satisfied $\langle x^4 \rangle = \int P(x)x^4 dx = \mu^4 + 6\mu^2\sigma^2 + 3\sigma^2\sigma^2$, with a relative error smaller than 5%, (where $\mu = \langle x \rangle$ denotes the mean and $\sigma^2 = \langle x^2 \rangle - \langle x \rangle^2$ the variance), indicating that the distributions are well approximated by Gaussians.

We address here how random fluctuations in neural activity (independent of the learned patterns) affect the performance of the familiarity discriminators. We study the effect of temperature at two different time points, $t = 0$ and $t = 1$. As stated above, time is defined such that in one unit, all neurons are asynchronously updated once. The choice of $t = 1$ is not special; we just study the network properties at this time to gain understanding as to how the network evolves.

The results are illustrated in figure 2. Immediately after stimulus ($t = 0$), we observe that FamE is independent of the temperature value (figure 2.A), whilst FamS has a non-linear dependence on the temperature (figure 2.C). For high temperature, FamS performs better as a familiarity discriminator. This finding can be intuitively understood. The energy and its time derivative can be separated into signal and noise contributions. The signal for the slope is proportional to the rate of change of the energy, and therefore proportional to the rate of change of the overlap between the network activity and the stimulus. At low temperatures, the signal associated with an old stimulus is very low as the overlap with the stimulus is almost invariant.

Contrarily, at higher temperature, the overlap with old stimuli changes very quickly; it decays from 1 to 0, and consequently the slope-signal relationship increases considerably (the higher temperature, the higher signal for FamS). The noise component for the slope, although dependent on T , is similar for both old and novel stimuli. As a result the main temperature dependence stems from the signal term. In figure 2, the case of $T > 1$ is not explicitly studied because in this region the network can not retrieve any of the learned patterns, i.e. the only stable solution is $\mathbf{m} = 0$, what is so-called *paramagnetic* or *non-memory* solution (Amit, 1989).

(FIGURE 2 HERE)

In contrast to time $t = 0$, at time $t = 1$, post stimulus presentation, both discriminators FamE and FamS show a similar breakdown in discrimination for increased temperature (figure 2.F). In the next section, we analytically study the maximum storage capacity for both FamE and FamS at time $t = 0$. The results are in agreement with the simulations. For $t = 1$, the mean field predictions, however, do not reproduce the network simulations. To study such situations (which we do not explicitly deal with here), one would need to use other techniques, for example, generating functional analysis (Coolen, 2001).

Maximum storage capacity

When the number of stimuli encoded in the weights increases, the SNR decreases. One can define the storage capacity (or maximum number of stimuli encoded in the learning rule and successfully discriminated) as the point where the SNR drops below one. This gives the maximum number of

stimuli M_{\max} that can be encoded in the network. In this section we present explicit calculations for both discriminators FamE and FamS for time $t = 0$.

Storage capacity of FamE

Let $\rho = \hat{\rho}$ label an old stimulus presented to the network. As is common in these calculations (Herz et al., 1991), we separate the sum appearing in equation (3) into a signal ($\rho = \hat{\rho}$) plus noise contributions. The latter is determined by interference from previously stored stimuli ($\rho \neq \hat{\rho}$). From equation (5) it follows that the energy associated with old stimuli is distributed as

$$E_{\text{old}}(t) = -N[m^{\hat{\rho}}(t)]^2 - N \sum_{\rho \neq \hat{\rho}} [m^{\rho}(t)]^2. \quad (9)$$

The first term on the right hand side is the signal and the second one the noise contribution. At $t = 0$, we obtain $m^{\hat{\rho}}(t = 0) = 1$ because the pattern $\hat{\rho}$ was an old stimulus. As for large N the central limit theorem applies, the overlaps with the other patterns $\rho \neq \hat{\rho}$ have a Gaussian distribution with 0 average and variance $1/N$ (Amit et al., 1987). Accordingly, we can easily compute the expected value and the variance for the energy. Using that the sum of two Gaussian distributed variables is again a Gaussian distribution,

$$E_{\text{old}}(t = 0) \in \mathcal{N}[-(N + M), 2M]. \quad (10)$$

Analogously, the energy for novel stimuli is distributed as

$$E_{\text{new}}(t = 0) \in \mathcal{N}[-M, 2M]. \quad (11)$$

From equation (8) we obtain $\text{SNR} = \sqrt{N^2/(2M)}$, in agreement with the simulations (see figure 2.E). Equivalently, the maximum storage capacity,

(the M for which $\text{SNR} = 1$), is given by

$$M_{\max}[\text{FamE}, t = 0] = \frac{N^2}{2}, \quad (12)$$

and thus the storage is of order N^2 , which has been reported in previous computational models using FamE (Bogacz and Brown, 2003).

Storage capacity of FamS

Following the same strategy applied to FamE to FamS, we are able to separate signal ($\rho = \hat{\rho}$) and noise ($\rho \neq \hat{\rho}$) terms for the slope. At the instant of the stimulus presentation ($t = 0$), we substitute equation (7) in equation (6). Next, we apply the central limit theorem, which is a good approximation for large N . It ensures that the sum over the different sites i of the noise contribution $\sum_{\rho \neq \hat{\rho}} x_i^\rho m^\rho$ appearing inside the tanh function, is equivalent to the average over a Gaussian noise with mean 0 and variance $\alpha \equiv M/N$, the network *load*. Using these considerations, it is straightforward to obtain

$$S_{\text{old}}(t = 0) \in \mathcal{N}[2N(1 - I_1 - I_2) + 2M, 8M], \quad (13)$$

and for novel stimuli

$$S_{\text{new}}(t = 0) \in \mathcal{N}[-2NI_3 + 2M, 8M]. \quad (14)$$

The integrals I_1 , I_2 and I_3 appearing in equations (13) and (14) are

$$\begin{aligned} I_1(\alpha, \beta) &\equiv \int \frac{dz}{\sqrt{2\pi}} \exp(-z^2/2) \tanh(\beta + \beta\sqrt{\alpha}z), \\ I_2(\alpha, \beta) &\equiv \int \frac{dz}{\sqrt{2\pi}} \exp(-z^2/2) \tanh(\beta + \beta\sqrt{\alpha}z) \sqrt{\alpha}z, \\ I_3(\alpha, \beta) &\equiv \int \frac{dz}{\sqrt{2\pi}} \exp(-z^2/2) \tanh(\beta\sqrt{\alpha}z) \sqrt{\alpha}z, \end{aligned} \quad (15)$$

where $\beta \equiv 1/T$ is the inverse temperature. From equations (13) and (14) it follows that $\text{SNR} = \sqrt{N^2/(2M)}[1 - I_1(\alpha, \beta) - I_2(\alpha, \beta) + I_3(\alpha, \beta)]$, which can be computed numerically. The results are represented in figure 2.E. The expected values used in the signal-to-noise ratio calculation (figure 2.C) fits well with the simulations. However, the theoretical predictions for the variance of both FamS(old) and FamS(new) equals $8M$, independent of temperature, which is in disagreement with the simulations. Therefore, the signal-to-noise ratio calculation disagrees with simulations for high temperatures (figure 2.E). See the appendix for a more detailed calculation of how the mean field prediction is affected by high temperatures.

(FIGURE 3 HERE)

The maximum storage for FamS is again obtained by solving $\text{SNR} = 1$, which yields

$$M_{\max}[\text{FamS}, t = 0] = \frac{N^2}{2}(1 - I_1(\alpha_{\max}, \beta) - I_2(\alpha_{\max}, \beta) + I_3(\alpha_{\max}, \beta))^2. \quad (16)$$

Because the integrals $I_1(\alpha, \beta)$, $I_2(\alpha, \beta)$ and $I_3(\alpha, \beta)$ depend on M , this expression does not give us M_{\max} explicitly. The dependence on N is more complicated than for other computational models of familiarity discrimination (Bogacz and Brown, 2003), (and in particular for FamE above), for which the maximum storage capacity is directly proportional to N^2 . Interestingly, M_{\max} for FamS at $t = 0$ is dependent on the temperature, whilst FamE is completely independent of temperature (recall figure 2, graphs A and C).

In the two limits $T = 0$ and $T \rightarrow \infty$ we can perform the integrals in equation (16) to obtain M_{\max} explicitly. For $T = 0$, the integrals (15) can

be computed using

$$\begin{aligned}\lim_{\beta \rightarrow \infty} \int \frac{dz}{\sqrt{2\pi}} \exp(-z^2/2) \tanh(\beta[az+b]) &= \operatorname{erf}\left(\frac{b}{\sqrt{2a}}\right), \\ \lim_{\beta \rightarrow \infty} \int \frac{dz}{\sqrt{2\pi}} \exp(-z^2/2) \tanh(\beta[az+b]) z &= \sqrt{\frac{2}{\pi}} \exp\left(-\frac{b^2}{2a^2}\right),\end{aligned}\quad (17)$$

giving $\lim_{\beta \rightarrow \infty} I_1(\alpha, \beta) = \operatorname{erf}\left(\frac{1}{\sqrt{2\alpha}}\right)$, $\lim_{\beta \rightarrow \infty} I_2(\alpha, \beta) = \sqrt{\frac{2\alpha}{\pi}} \exp\left(-\frac{1}{2\alpha}\right)$ and $\lim_{\beta \rightarrow \infty} I_3(\alpha, \beta) = \sqrt{\frac{2\alpha}{\pi}}$. Here, $\operatorname{erf}(x)$ is the error function $\operatorname{erf}(x) \equiv \frac{2}{\sqrt{\pi}} \int_0^x \exp(-u^2) du$. Therefore at $T = 0$ equation (16) becomes

$$M_{\max} = \frac{N^2}{2} \left(1 - \operatorname{erf}\left(\sqrt{\frac{N}{2M_{\max}}}\right) + \sqrt{\frac{2M_{\max}}{\pi N}} \left[1 - \exp\left(-\frac{N}{2M_{\max}}\right) \right] \right)^2. \quad (18)$$

In figure 3 we plot, as a function of N , the ratio of the initial zero temperature storage for FamS and FamE. We see that although FamS performs slightly worse than FamE, both storage capacities grow proportional to N^2 . By way of example, for $N = 1000$, we see $M_{\max}[\text{FamS}, t = 0, T = 0] \approx 96\% M_{\max}[\text{FamE}, t = 0]$, i.e. the capacities are almost identical.

In the other limit that $T \rightarrow \infty$, random fluctuations in neural activity dominate the network dynamics. All the integrals of (15) are zero, and hence $M_{\max}[\text{FamS}, t = 0] \approx M_{\max}[\text{FamE}, t = 0]$. That is, in this limit, the theoretical maximum storage is the same for both FamS and FamE, and is independent of T .

Discussion

Familiarity describes a retrieval process that supports recognition memory by providing a feeling that something has been encountered before. Numerous empirical studies have investigated familiarity processes in humans

(Yonelinas, 2002) and non-humans (Brown and Xiang, 1998). Recently, some neuronal networks modeling familiarity discrimination have also been proposed (Bogacz and Brown, 2003). However, no computational work has addressed the dynamics of familiarity discrimination, which is relevant when comparing these models to experiments. Furthermore, we have studied how noise affects the familiarity performance.

We have compared the energy discriminator (FamE) used by (Bogacz and Brown, 2003) to its time derivative, the slope (FamS). Interestingly, the FamS discriminator was already suggested by Hopfield in his seminal work (Hopfield, 1982). An interesting consequence is that the original Hopfield model can be used to model both recollection (stationary properties of the retrieval dynamics) and familiarity (transient dynamics after the stimulus presentation). The slope discriminator (FamS) is affected by the temporal dependency of the energy discriminator (FamE). In other words, the slope discriminator captures the fact that the speed of discrimination is predictive for the discrimination outcome *per se*.

For both discriminators the familiarity signals decay quickly after stimulus presentation and are detectable only for a short period of time. This can be compared to the speed of recollection. Assuming that recollection memories correspond to attractors in the Hopfield model, recollection information only becomes available once the attractor state is reached. By that time, the slope is zero, and the energy difference is very small. Thus the experimentally observed timing difference of familiarity and recollection follows naturally from our model.

The storage capacity of these familiarity discriminators is much larger (proportional to N^2) compared to recollection (proportional to N), we demonstrated that this capacity is dependent on the *temperature*. We have pre-

sented a detailed derivation of the maximum storage immediately after stimulus presentation ($t = 0$). We have shown that for low temperature, the storage capacity related to FamS is lower than that for FamE, but still scales with the number of synapses, e.g. for $N = 1000$, the slope gives a storage capacity 96% as good as the energy. For high temperatures the difference between the storage capacities of FamS and FamE is negligible (the storage capacity for both is the approximately, $N^2/2$).

Interestingly, this means that the performance of FamS improves as one goes to the high temperature regime, a fact which is a priori counterintuitive, especially given how the temperature affects *recollection* in Hopfield nets (Amit, 1989), i.e. the higher the temperature, the worse the recollection performance. However, after some time steps, our simulations (figure 2.F) show that, for both FamE and FamS, high noise levels produce a stochastic disruption of the discrimination, decreasing the SNR and the performance of familiarity, a concurrence with the dynamics of recollection.

Acknowledgments

The authors acknowledge Rafal Bogacz (Univ. Bristol) and David Donaldson (Univ. Stirling) for helpful discussions and financial support from EPSRC (project Ref. EP/CO 10841/1), HFSP (project Ref. RGP0041/2006) and from the Doctoral Training Center in Neuroinformatics at the University of Edinburgh.

Appendix: Mean field validity dependence on temperature

To compute the slope in equation (6), we need an analytic expression for dm^p/dt , or equivalently, given the definition (4), we have to compute the derivative ds_i/dt , which is governed by the Glauber dynamics given by (2),

see (Marro and Dickman, 1999) for more detailed situations. Given $s_i(t)$, the Glauber dynamics give an uncertainty in $s_i(t+1)$, such that

$$\text{Var}[s_i(t+1)|\{s_j(t)\}] = \text{sech}^2(\beta h_i(t)), \quad (19)$$

which implies

$$\frac{ds_i}{dt} = \tanh(\beta h_i) - s_i + \mathcal{O}(\text{sech}(\beta h_i)). \quad (20)$$

We use this result to find the error induced in our calculation of S_{new} . When a new pattern is presented, the m^ρ are all of order $N^{-1/2}$. This implies that the local fields, defined as $h_i \equiv \sum_\rho x_i^\rho m^\rho$, are of order $\sqrt{\alpha} \equiv \sqrt{M/N}$. Hence, by equations (4) and (20), the error in our calculation of dm^ρ/dt is given by

$$\text{Error} \left(\frac{dm^\rho}{dt} \right) = \mathcal{O} \left(\frac{1}{\sqrt{N}} \text{sech}(\beta \sqrt{\alpha}) \right), \quad (21)$$

for each ρ . Finally, by (6), we conclude that

$$\text{Error}(S_{\text{new}}) = \mathcal{O} \left(\sqrt{M} \text{sech} \left(\frac{1}{T} \sqrt{\frac{M}{N}} \right) \right). \quad (22)$$

Since $\text{sech}(x)$ decays exponentially with large x , but is of order 1 for small x , the error in our calculation of S_{new} , coming from the mean field approximation, is only going to be negligible in the limit in which $(1/T)\sqrt{M/N}$ is large. This explains why there is a growing discrepancy between theory and simulation as the temperature T is increased (see figure 2.E).

References

- J.P. Aggleton and M.W. Brown. Contrasting hippocampal and perirhinal cortex function using immediate early gene imaging. *Q J Exp Psychol B*, 58:218–233, 2005.
- D.J. Amit. *Modeling brain function: The world of attractor neural networks*. Cambridge University Press, 1989.
- D.J. Amit, H. Gutfreund, and H. Sompolinsky. Statistical mechanics of neural networks near saturation. *An Phys*, 173:30–67, 1987.
- R. Bogacz and M.W. Brown. Comparison of computational models of familiarity discrimination in the perirhinal cortex. *Hippocampus*, 13:494–524, 2003.
- M.W. Brown and J.P. Aggleton. Recognition memory: What are the roles of the perirhinal cortex and hippocampus? *Nat Rev Neurosci*, 2:51–61, 2001.
- M.W. Brown and J.Z. Xiang. Recognition memory: neuronal substrates of the judgment of prior occurrence. *Prog Neurobiol*, 55:149–189, 1998.
- M.W. Brown, F.A.W. Wilson, and I.P. Riches. Neuronal evidence that inferomedial temporal cortex is more important than hippocampus in certain processes underlying recognition memory. *Brain Res*, 409:158–162, 1987.
- A.C.C. Coolen. *Statistical Mechanics of Recurrent Neural Networks II: Dynamics*, volume 4, chapter 15, pages 597–662. Elsevier Science B.V., 2001.
- B.A. Doshier. Discriminating preexperimental (semantic) from learned (episodic) associations: a speed-accuracy study. *Cogn Psychol*, 16:519–555, 1984.

- A. Greve, M.C.W. van Rossum, and D.I. Donaldson. Investigating the functional interaction between semantic and episodic memory: Convergent behavioral and electrophysiological evidence for the role of familiarity. *Neuroimage*, 34(2):801–814, Jan 2007.
- J. Herz, A. Krogh, and R.G. Palmer. *Introduction to the theory of neural computation*. Addison-Wesley Longman, 1991.
- J.J. Hopfield. Neural Networks and Physical Systems with Emergent Collective Computational Abilities. *Proc Natl Acad Sci USA*, 79:2554–2558, 1982.
- J. Marro and R. Dickman. *Nonequilibrium Phase Transitions in Lattice Models*. Cambridge University Press, 1999.
- A.V. Robins and S.J.R. McCallum. A robust method for distinguishing between learned and spurious attractors. *Neural Netw*, 17:313–326, 2004.
- M.D. Rugg and A.P. Yonelinas. Human recognition memory: a cognitive neuroscience perspective. *Trends Cogn Sci*, 7:313–319, 2003.
- M.D. Rugg, R.E. Mark, P. Walla, A.M. Schloerscheidt, C.S. Birch, and K. Allan. Dissociation of the neural correlates of implicit and explicit memory. *Nature*, 392:595–598, 1998.
- L. Standing. Learning 10000 pictures. *Q J Exp Psychol*, 25:207–222, 1973.
- A.P. Yonelinas. The nature of recollection and familiarity: A review of 30 years of research. *J Mem Lang*, 46:441–517, 2002.

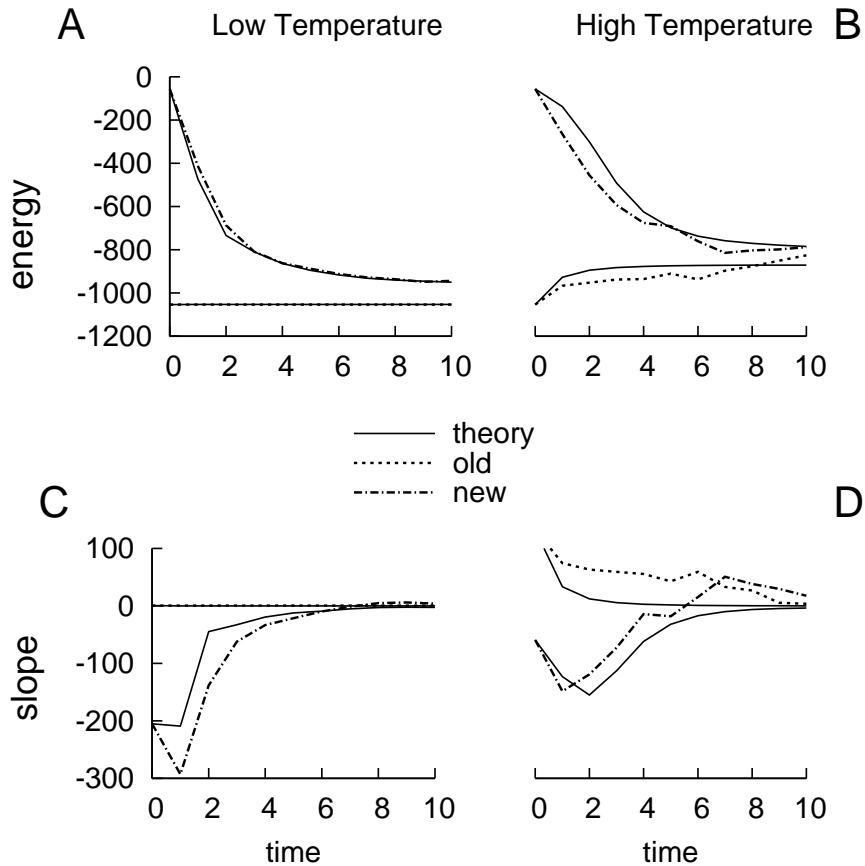


Figure 1: **Temporal persistence of discrimination by familiarity.** For different values of the temperature parameter, $T = 0.20$ on the left and $T = 0.60$ on the right, we simulate a network of $N = 1000$ neurons and $M = 50$ uncorrelated patterns. Both FamE and FamS can discriminate between novel and old stimuli during a short period post stimulus presentation. After this, the slope begins to tend to zero, indicating that the activity has converged to one of the stored stimuli. This is due to the well-known pattern completion dynamics that occurs in attractor neural networks. One unit of time is defined as the time taken to update the whole population of neurons in the network.

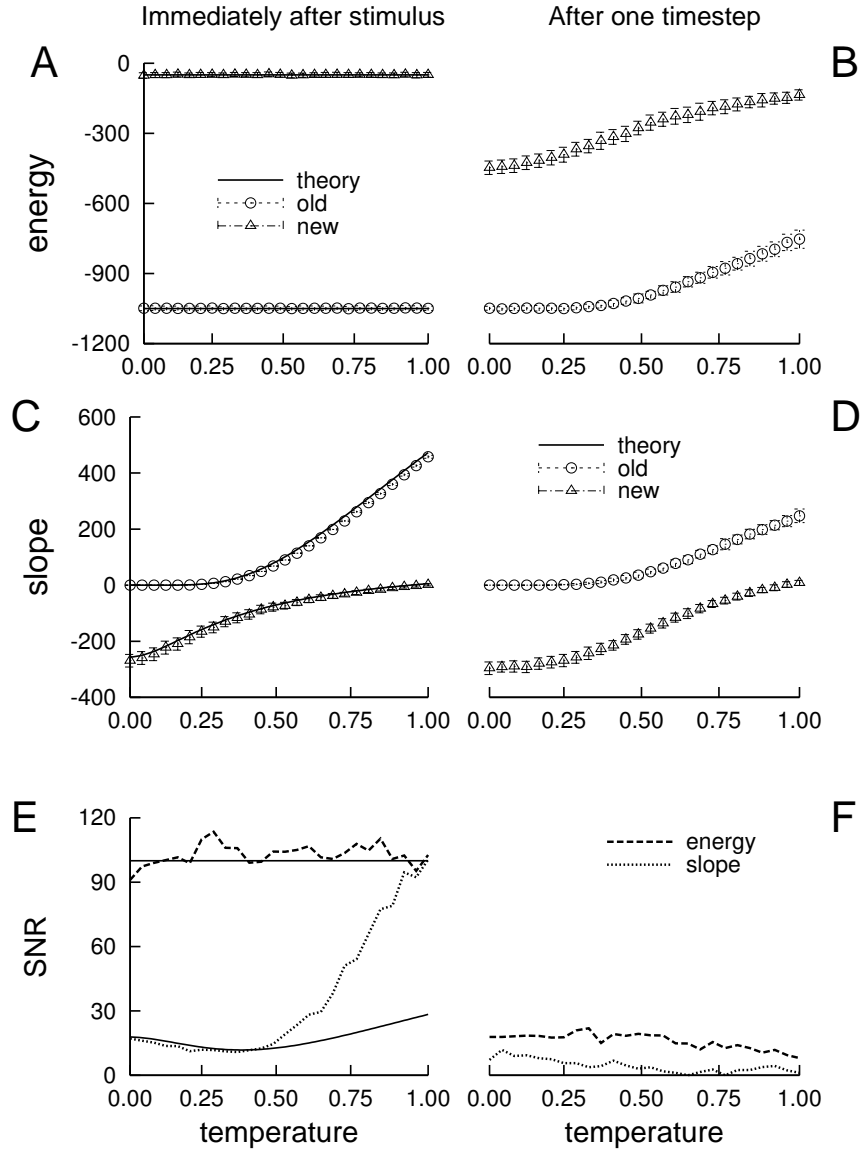


Figure 2: **Robustness of discrimination by familiarity.** Immediately after stimulus presentation, left graphs, FamE is independent of temperature, whereas FamS is enhanced if the temperature parameter increases. After one timestep, right graphs, both FamE and FamS deteriorate for high values of temperature. We represent the values of the energy (top graph) and the slope (middle) with the standard deviation. On the bottom, each point in the curves corresponds with a fixed value of temperature, in which we compute the SNR concerning the probability distributions of the network responses towards both familiar and novel stimuli. These simulations correspond with averaging over 100 runs of a network with $N = 1000$ neurons and $M = 50$ uncorrelated patterns. Black solid lines are the theoretical predictions (see text for details).

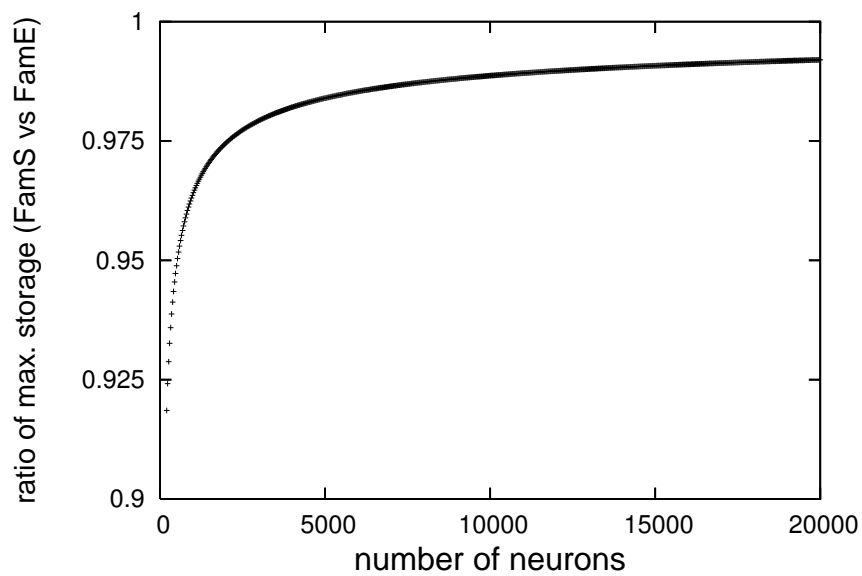


Figure 3: **Ratio of initial storage capacities at zero temperature.** The storage of discriminator FamS is obtained by numerical solution of equation (18) as a function of the number of neurons N . This is normalized by the storage for FamE (12), to obtain a ratio of the performances of the two discriminators.